Electronic Supplementary Material (ESI) for Industrial Chemistry & Materials.

Mono-, bi- and tri-metallic platinum group metal-free electrocatalyst for hydrogen evolution reaction following a facile synthetic route

Seyed Ariana Mirshokraee,[a] Mohsin Muhyuddin,[a] Jacopo Orsilli,[a] Enrico Berretti,[b] Laura Capozzoli,[b] Alessandro Lavacchi,[b] Carmelo Lo Vecchio,[c] Vincenzo Baglio,[c] Anna Galli,[a] Andrea Zaffora,[d] Francesco Di Franco,[d] Monica Santamaria,[d] Luca Olivi,[e] Simone Pollastri[ef] and Carlo Santoro*[a]

[a] Department of Materials Science, University of Milano-Bicocca, U5, Via Cozzi 5, 20125, Milano, Italy
[b] Istituto di Chimica Dei Composti OrganoMetallici (ICCOM), Consiglio Nazionale Delle Ricerche (CNR), Via Madonna Del Piano 10, 50019 Sesto Fiorentino, Firenze, Italy
[c] Istituto di Tecnologie Avanzate per l'Energia "Nicola Giordano" (ITAE), Consiglio Nazionale delle Ricerche (CNR), Via Salita S. Lucia sopra Contesse 5, Messina, 98126, Italy
[d] Department of Engineering, University of Palermo, Viale delle Scienze, 90128, Palermo, Italy
[e] Elettra-Sincrotrone Trieste, Area Science Park, Basovizza, Trieste, Italy
[f] Department of Physics, Computer Science and Mathematics, University of Modena and Reggio Emilia, Via Campi 103, 41125 Modena, Italy

*Corresponding author: carlo.santoro@unimib.it

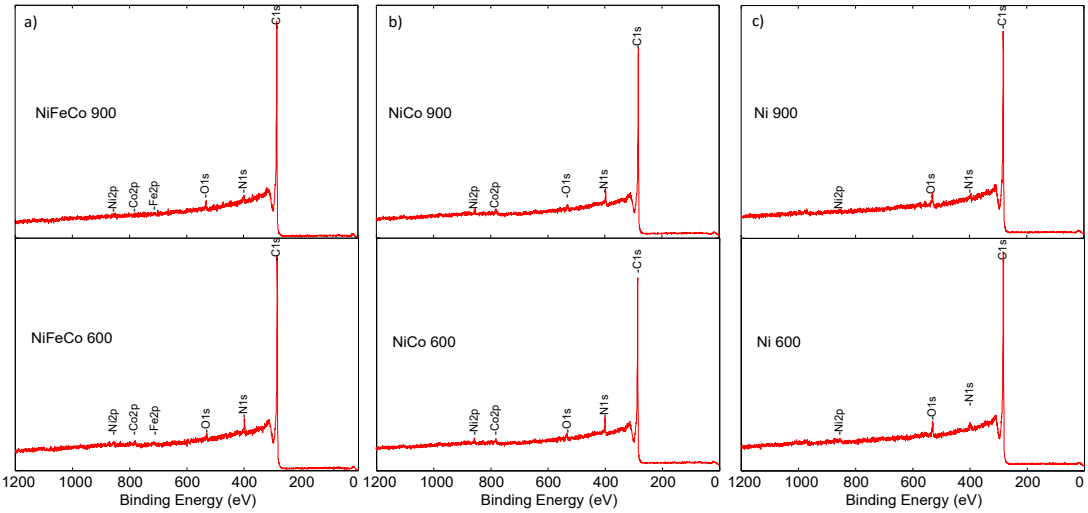

Figure S1: XPS survey spectra for a) Ni-Fe-Co 600 and Ni-Fe-Co 900, b) Ni-Co 600 and Ni-Co 900 and c) Ni 600 and Ni 900.

Table S1. Atomic percentage of C1s, N1s, Fe2p3, Co2p3, Ni2p3 and O1s in the electrocatalysts derived from XPS analyses.

	Carbon C1s	Nitrogen N1s	Iron Fe2p3	Cobalt Co2p3	Nickel Ni2p3	Oxygen O1s
Ni-Fe-Co 600	93.8	5.1	0.3	<0.1	0.1	0.6
Ni-Fe-Co 900	96.6	1.8	0.2	<0.1	0.1	1.4
Ni-Co 600	92.9	4.5	-	0.4	<0.1	2.3

Ni-Co 900	97.3	1.1	-	<0.1	0.3	1.3
Ni 600	94.4	2.4	-	-	0.2	3.0
Ni 900	95.7	1.1	-	-	0.3	3.0

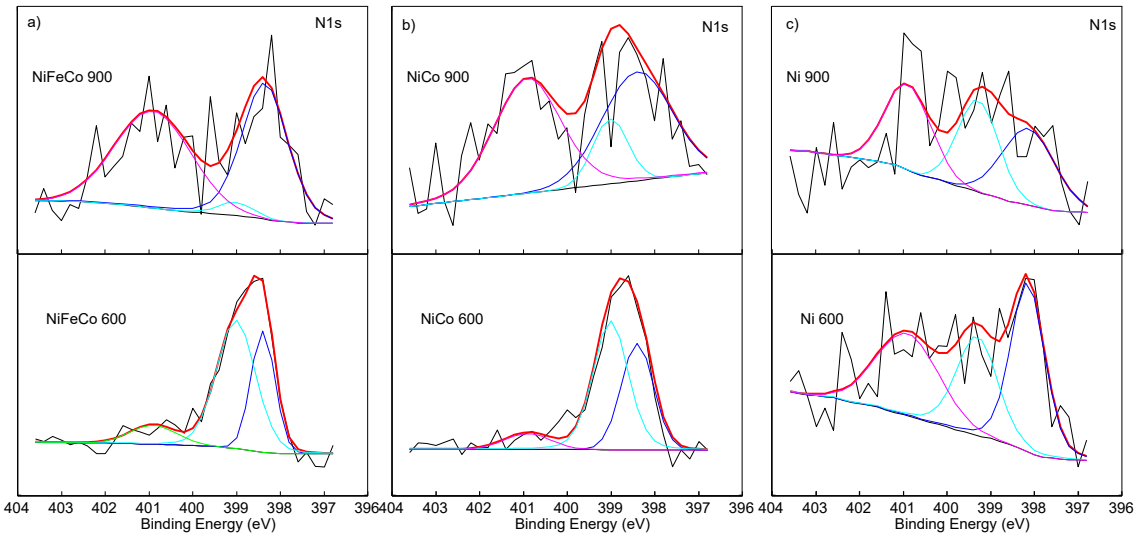

Figure S2: Comparison of XPS N1s signal for a) Ni-Fe-Co 600 and Ni-Fe-Co 900, b) Ni-Co 600 and Ni-Co 900 and c) Ni 600 and Ni 900.

Table S2: Composition of N (relative %)

Composition of N (relative %)							
Electrocatalysts	N (at. %)	Imine	Pyridinic (398.2 eV)	N-M (M=Fe, Co, Ni) 399.1 eV ± 0.1	Pyrrolic (400.9 eV)	Graphitic	N-O
Ni-Fe-Co 600	5.1	-	32.1	58.2	9.7	-	-
Ni-Fe-Co 900	1.8	-	46.3	3.5	50.2	-	-
Ni-Co 600	4.5	-	37.7	54.2	8.1	-	-
Ni-Co 900	1.1	-	41.7	12.6	45.7	-	-
Ni 600	2.4	-	39.5	27.9	32.6	-	-
Ni 900	1.1	-	34.3	32.0	33.7	-	-

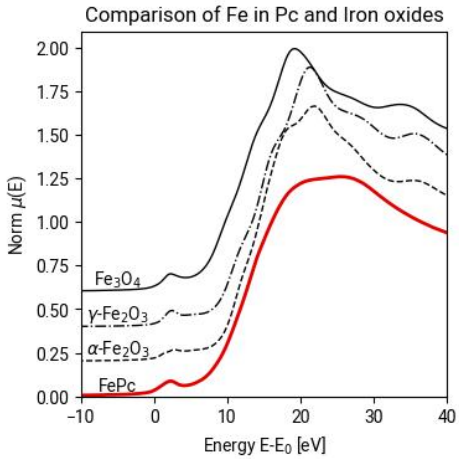

Figure S3. Comparison of the normalized XANES spectra of iron in the Ni-Co-Fe electrocatalysts at room temperature, red, and different Fe^{3+} oxides reference spectra (from the beamline database), which present the same pre-edge peak structure.

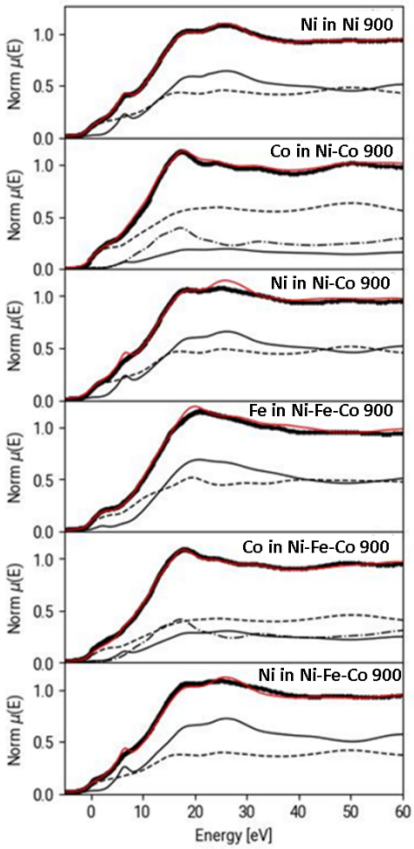

Figure S4. LCF of the different XANES spectra collected on the pyrolyzed samples. Black thick lines for the experimental data, red lines for the fitted profile, dashed lines for the metal reference, solid black lines are the heated phthalocyanine spectra, and dot-dashed lines the metal oxide.

Table S3. Best-fit weights were obtained with the LCF analyses of the pyrolyzed Ni-based electrocatalysts.

Sample and TM	% Components		
	Metallic	Pc at 600°C	Oxide
Ni in Ni 900	46.4±0.6	53.6±0.6	-
Co in Ni-Co 900	57.1±1.2	16.2±1.4	26.7±1.9
Ni in Ni-Co 900	46.9±1.3	53.1±1.3	-
Fe in Ni-Fe-Co 900	46.2±1.5	53.8±0.8	-
Co in Ni-Fe-Co 900	45.5±0.8	26.3±1.0	28.1±1.3
Ni in Ni-Fe-Co 900	40.3±1.3	59.7±1.3	-

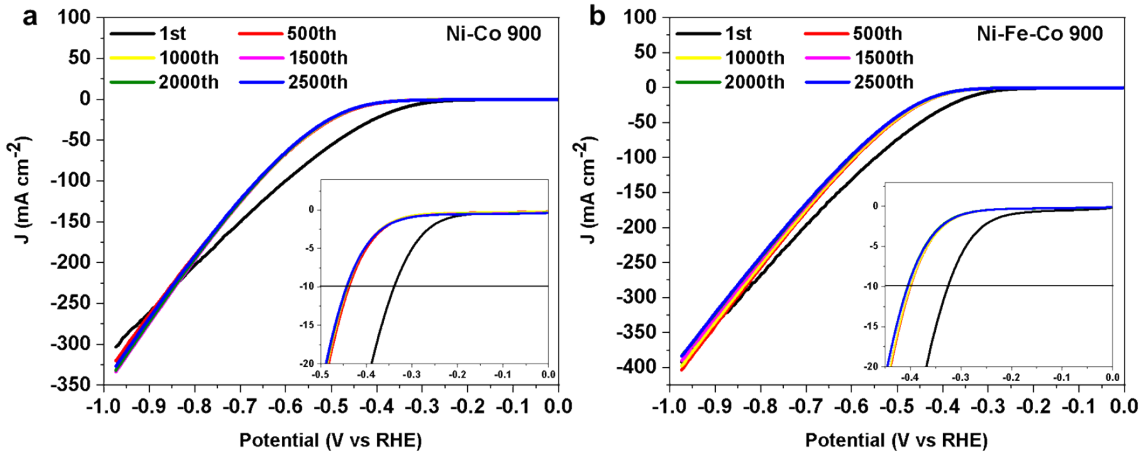

Fig. S5: HER stability test (2500 cycles) on (a) Ni-Co 900 electrocatalyst and (b) Ni-Fe-Co 900 electrocatalyst

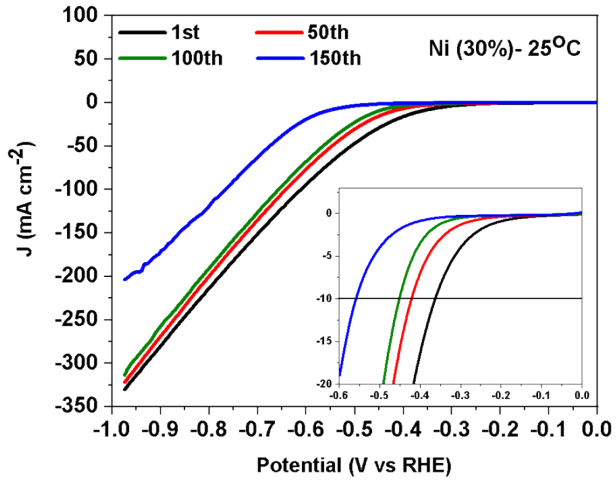

Fig. S6: HER stability test (150 cycles) on (a) Ni (30%) without thermal treatment (25°C)

Table S4. Performance comparison with other literature

Electrocatalyst	Overpotential at 10 mA cm^{-2} (mV)	Electrolyte	Mass loading (mg cm^{-2})	Ref.
$NiFeO_x$ NPs	88	1 M KOH	1.6	[1]
Co-Ni_3N NWs	194	1 M KOH	2.91	[2]
Ni−P NSs	117	1 M KOH	0.3	[3]
Ni-N-C	307	1 M KOH	-	[4]
NiNC_P	403	1 M KOH	0.6	[5]
NiCoOS	300	0.1 M KOH	0.3	[6]
MnNiCo-P	288	1 M KOH		[8]
Fe-Ni@NCF	219	1 M KOH		[9]
Ni_7Co_3/NC-500	90	1 M KOH		[10]
carbon cage-encapsulated FeNiMo	199	1 M KOH		[11]
Ni900, Ni-Fe-Co900, and Ni-Fe-Co600	320	1 M KOH	0.6	This work

Table S5.: Summary of all the relevant morphological and analytical observations for Ni based electrocatalysts.

Sample	Overpotential (V)	Average particle size (nm)	I_D/I_G	main particle form	XRD peaks (^{o})
Ni 900	0.32	26	1.2	Metal-oxide	24, 43, 44.2, 51.5
Ni 600	0.34	45	1.3	metallic	24, 43, 44.2, 51.5
Ni-Co 900	0.34	36	1.6	Ni-Co alloy oxide	24, 43, 44.3, 51.2, 75
Ni-Co 600	0.34	5	0.75	Ni-Co alloy oxide	24, 43
Ni-Fe-Co 900	0.32	15 - 60	1.5	Ni-Fe-Co alloy	24, 43, 43.6, 51, 75
Ni-Fe-Co 600	0.32	28	0.9	Fe oxide	24, 43

References

1. Wang, H.; Lee, H.-W.; Deng, Y.; Lu, Z.; Hsu, P.-C.; Liu, Y.; Lin, D.; Cui, Y. Bifunctional Non-Noble Metal Oxide Nanoparticle Electrocatalysts Through Lithium-Induced Conversion for Overall Water Splitting. Nat. Commun. 2015, 6, 7261.
2. Zhu, C.; Wang, A.-L.; Xiao, W.; Chao, D.; Zhang, X.; Tiep, N. H.; Chen, S.; Kang, J.; Wang, X.; Ding, J.; et al. In Situ Grown Epitaxial Heterojunction Exhibits High-Performance Electrocatalytic Water Splitting. Adv. Mater. 2018, 30, 1705516.
3. Wang, X.; Li, W.; Xiong, D.; Petrovykh, D. Y.; Liu, L. Bifunctional Nickel Phosphide Nanocatalysts Supported on Carbon Fiber Paper for Highly Efficient and Stable Overall Water Splitting. Adv. Funct. Mater. 2016, 26, 4067−4077.
4. Lei C, Wang Y, Hou Y, et al. Efficient alkaline hydrogen evolution on atomically dispersed Ni–N x Species anchored porous carbon with embedded Ni nanoparticles by accelerating water dissociation kinetics. *Energy & Environmental Science*. 2019;12(1):149-156. doi:10.1039/C8EE01841C
5. Muhyuddin M, Zocche N, Lorenzi R, et al. Valorization of the inedible pistachio shells into nanoscale transition metal and nitrogen codoped carbon-based electrocatalysts for hydrogen evolution reaction and oxygen reduction reaction. *Mater Renew Sustain Energy*. 2022;11(2):131-141. doi:10.1007/s40243-022-00212-5
6. Bai Z, Li S, Fu J, et al. Metal-organic framework-derived Nickel Cobalt oxysulfide nanocages as trifunctional electrocatalysts for high efficiency power to hydrogen. *Nano Energy*. 2019;58:680-686. doi:10.1016/j.nanoen.2019.01.050
7. Salem KE, Saleh AA, Khedr GE, Shaheen BS, Allam NK. Unveiling the Optimal Interfacial Synergy of Plasma-Modulated Trimetallic Mn-Ni-Co Phosphides: Tailoring Deposition Ratio for Complementary Water Splitting. *Energy and Environmental Materials*. doi:10.1002/eem2.12324

8. Zhang Z, Cong L, Yu Z, Qu L, Huang W. Facile synthesis of Fe–Ni bimetallic N-doped carbon framework for efficient electrochemical hydrogen evolution reaction. Materials Today Energy. 2020 Jun 1;16:100387.
9. Hu L, Shi J, Peng Z, Zheng Z, Dong H, Wang T. A high-density nickel–cobalt alloy embedded in nitrogen-doped carbon nanosheets for the hydrogen evolution reaction. Nanoscale. 2022;14(16):6202–11.
10. Zhang Z, Cong L, Yu Z, Qu L, Qian M, Huang W. FeNiMo trimetallic nanoparticles encapsulated in carbon cages as efficient hydrogen evolution reaction electrocatalysts. Materials Advances. 2020;1(1):54–60.